ELSEVIER

Dielectric Amplification in Cement Pastes

S.J. Ford, J.-H. Hwang, J.D. Shane, R.A. Olson, G.M. Moss, H.M. Jennings, and T.O. Mason

Dielectric amplification (dielectric constants >80) is observed in cement pastes at early ages. Standard nonlinear least squares fitting routines yield artificially large "capacitances" when constant phase elements are employed. Instead, capacitance vs. frequency analysis provides reliable evidence of dielectric amplification. A physical model system consisting of a polycarbonate box with electrodes at each end, divided into two compartments by a polycarbonate barrier with a single hole, and filled with electrolyte solution, simulates the impedance response in young cement pastes. The barrier represents hydration products whereas the hole represents the constriction between two adjacent capillary pores, i.e., the pore network remains percolated. Dielectric amplification is inversely proportional to barrier thickness, i.e., it decreases as the barrier (product phase) thickens. Impedance spectra from real pastes vs. water/cement (w/c) ratio and during freezing or solvent exchange (to preferentially reduce the conductivity of the capillary pores) exhibit significant dielectric amplification, even after freezing or exchange, suggesting that C-S-H gel also has a dielectrically amplified microstructure. ADVANCED CEMENT BASED MATERIALS 1997, 5, 41–48. *© 1997 Elsevier Science Ltd.*

KEY WORDS: Dielectric amplification, Impedance spectroscopy, Cement paste, Constricted microstructure, Percolation, Pore system, Dielectric constant.

Several groups have investigated the electrical response of cement-based systems as a noninvasive technique for monitoring the microstructural evolution of these materials [1–10]. Recently, the relative dielectric constant of cementitious materials (k_r) has been the focus of much attention, and values as large as 10^5 have been reported for cement pastes at early hydration times [1,4,11]. Cement paste can be described as a 3-3-0 electrocomposite having interconnected pore fluid and C-S-H gel phases (3D connectivity) and various other disconnected solid phases (0D connectivity) [12,13]. It has been shown that the highly conductive, continuous pore phase controls the conductivity of cement-based materials, being proportional to the volume fraction of pore fluid (ϕ), its conductivity (σ_o), and connectivity (β) [1,7]. Similarly, because the dielectric constant for the liquid phase is near 80, and is much larger than the dielectric constants of all other phases, the dielectric behavior of the bulk paste should be dominated by the amount of pore water in the system [4]. It can be assumed that the dielectric response is proportional to the volume fraction of porosity (ϕ) in saturated pastes. This is not borne out experimentally, however, as the reported values for the bulk dielectric constant appear to be much higher than that of the pore solution. Such high values have given rise to several theories to account for the enhanced dielectric behavior of these materials [4,5,10]. In this paper, we discuss this "dielectric amplification." The origin of this amplification is explained as a combination of analysis errors and microstructural effects. An explanation of the microstructural contribution is presented, based on simulations of a constricted pore system and experimental data from both frozen cement pastes and pastes whose pore solution has been exchanged with isoproponal.

Experimental

Simulations

As with the electrical conductivity of these materials, their dielectric constants may be related to the tortuosity of the liquid phase. To test the effect of a constricted microstructure on the dielectric response, a simplified experimental model was used. Containers, as shown in Figure 1, were constructed from polycarbonate with dimensions 25.4 × 25.4 × 100 mm. C-1018 steel plates, polished to 600 grit, were used as electrodes for the impedance measurements described below, and polycarbonate barriers of varying thickness were placed midway between them. Tap water was used as the system electrolyte, and the barriers, having the same cross-sectional area as the containers, constricted the current flow through a hole 2.5 mm in diameter that was drilled through their centers. Epoxy was used between the barriers and container walls to prevent leakage.

Cement Pastes

Cement pastes of various water/cement ratios (w/c) were prepared using ASTM Type I ordinary Portland

© 1997 by Elsevier Science Ltd.
655 Avenue of the Americas, New York, NY 10010

ISSN 1065-7355/97/$17.00
PII S1065-7355(96)00009-0

Advn Cem Bas Mat
1997;5:41–48

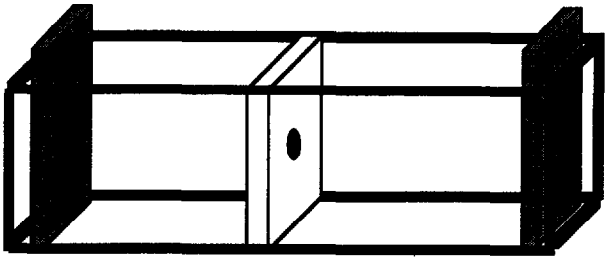

FIGURE 1. Schematic of the polycarbonate containers used to model constricted microstructures.

cement (OPC), mixed with distilled water for 15 minutes in a Hobart planetary mixer. The pastes were then cast into polycarbonate molds, similar to those described above, and stored in 100% relative humidity (RH) chambers. Details of the freezing and isopropanol exchange experiments, including specimen geometries and experimental procedures, are provided elsewhere [11,14].

Instrumentation

Impedance spectra were acquired using a Solartron 1260 frequency response analyzer (FRA) with "Z60" data collection software [15], over the frequency range 1 Hz to 10 MHz. An oscillating voltage of 25 mV was used as the excitation signal. Nulling procedures, described elsewhere [1], were used to remove inductive and capacitive effects from the leads and measurement apparatus, and the corrected spectra were analyzed using the "EQUIVCRT" software [16].

Results and Discussion

Dielectric amplification in cement-based materials is defined herein as the increase in the capacitance of the system above the values that would be expected if the volume fraction of pore solution, using the rule of mixtures, resulted in the dielectric response of the composite. The predicted capacitance values should be the product of the pore fluid capacitance and its volume fraction, expressed mathematically as:

$$C = \left[\frac{k_r(ps) \cdot A\varepsilon_o}{l}\right] \cdot \phi \qquad (1)$$

where C is the capacitance of the system, $k_r(ps)$ is the dielectric constant of the pore solution, A and l are the specimen area and length respectively, ϵ_0 is the permittivity of free space, and ϕ is the volume fraction of fluid filled porosity in the system. As discussed previously, capacitance values orders of magnitude higher than those predicted by Eq. 1 have been reported for cement pastes at early hydration times [1]. The present work addresses numerical fitting artifacts and possible microstructural origins of dielectric amplification.

Numerical Fitting

The first contribution to the reported dielectric amplification is the error introduced as a result of numerical fitting. Analysis and deconvolution of impedance spectra are usually accomplished with the aid of non-linear least squares (NLLS) fitting programs such as "EQUIVCRT" [17]. These programs allow the measured spectra to be fit to a user-defined equivalent circuit which simulates the impedance response of the system, and is composed of ideal circuit elements such as resistors, capacitors, and inductors. These circuit elements, if chosen correctly, represent various electrochemical processes, such as ionic conduction and dipole polarization occurring in the system. Because most systems are not ideal, these NLLS programs often allow non-ideal spectra to be fit with constant phase elements (CPEs). Figure 2 shows a numerically simulated, non-ideal response for the inset circuit combination. This equivalent circuit is a common representation for many electrochemical processes, and consists of a resistor in series with a resistor and non-ideal capacitor, or CPE, combined in parallel. The complex plane, or Nyquist plot in Figure 2 shows the characteristically depressed semi-circular arc for this circuit. The depression angle, θ, is a measure of the CPEs deviation from an ideal capacitor.

Constant phase elements are empirical functions having an impedance response of the form [17–19]:

$$Z(\text{CPE}) = B(j\omega)^{-n} \qquad (2)$$

or, separated into its real and imaginary components,

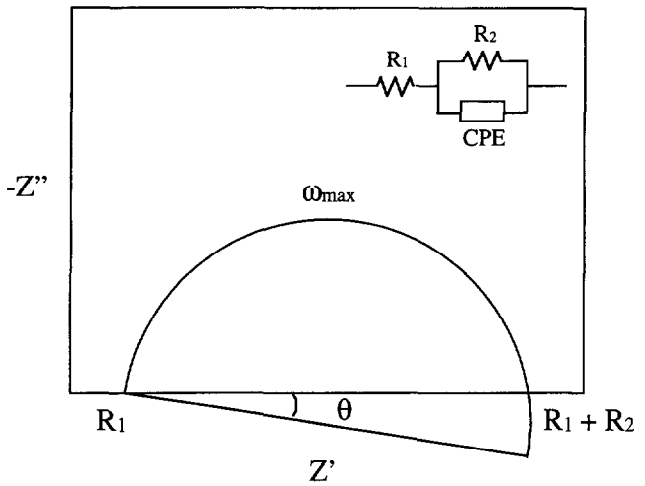

FIGURE 2. Schematic Nyquist plot for a resistor in parallel with a non-ideal capacitor.

$$Z(\text{CPE}) = B\omega^{-n}\left[\cos\left(\frac{n\pi}{2}\right) - j\sin\left(\frac{n\pi}{2}\right)\right] \quad (3)$$

where B is a constant, ω is the angular frequency, and n is a measure of arc depression having values between −1 and 1, which is related to the depression angle by the equation:

$$n = \left(1 - \frac{2\theta}{\pi}\right) \quad (4)$$

with θ in radians. Eq 3 is completely general and can be used to model all of the basic circuit elements, with variations only in their n-value, as shown in Table 1. Most often, CPEs are used to represent non-ideal capacitors to model depressed arcs in the complex impedance plane, as discussed above.

Cement-based materials usually produce semicircular impedance responses, similar to the depressed arc illustrated in Figure 2, where the CPE typically has n-values between 1 and 0.75, indicating predominately capacitive behavior. This depression of the impedance arc has been attributed to non-Debye behavior and a distribution of relaxation times in the system [18,19]. Regardless of the cause of the depression, this non-ideality can lead to misinterpretations of the system capacitance, as will be described below.

When constant phase elements are used to represent non-ideal capacitors, the inverse of the CPE constant, B from Eqs 2 and 3, is often the reported parameter. This "capacitive" constant Q, is defined as:

$$Q = B^{-1} \quad (5)$$

The constant Q is of interest because, when the n-value is equal to unity, Q is defined as the true, frequency independent, capacitance of the system. Because the real term of Eq 3 goes to zero as n approaches one, the impedance of the CPE becomes identical to that of a pure capacitor (see Table 1). Problems arise when Q is taken to be a true, single-valued capacitance for a non-ideal system, as the actual capacitance of the system may be orders of magnitude lower than Q. Fortunately, these misinterpretations are easily avoided because NLLS fitting procedures are unnecessary for obtaining capacitance information from experimental spectra.

Using the proper conversion factors [18], the measured impedance can directly give the capacitance of a system, without the need for numerical fitting. The impedance and capacitance values are related through the equation [18]:

$$\text{Re}(C) = \frac{-\text{Im}(Z)}{\omega\,|Z|^2} \quad (6)$$

where Re(C) is the real part of the capacitance, Im(Z) is the imaginary part of the impedance, ω is the angular frequency, and $|Z|$ is the total impedance given by:

$$|Z|^2 = [\text{Re}(Z)]^2 + [\text{Im}(Z)]^2 \quad (7)$$

This approach allows capacitance data to be directly obtained. It also highlights where errors in interpretation can be made.

Figure 3 shows the capacitance vs. frequency response of the inset equivalent circuit, simulated using the "EQUIVCRT" software. This equivalent circuit is a typical, although simplified, representation of cementitious systems, where the individual elements were assumed to have the values given in Table 2. The two curves differ only in the n-value assigned to the bulk CPE, as indicated in the figure, and thus in their deviation from ideality. The n = 1.0 curve is the ideal response, and the n = 0.75 curve is a non-ideal response. Because real systems are seldom ideal, the latter curve more closely resembles the response of typical cement-based systems [1]. At frequencies above approximately 10^4 Hz, these curves diverge owing to the difference in the bulk n-values. In this region misinterpretations are often made concerning the bulk capacitance of non-ideal materials systems. When n is equal to unity, as in the upper curve, Q is by definition the true capacitance of the bulk, and in this simulation would have a value of 10 nF (10^{-8}F). When n diverges from one as in the lower curve, it can be seen that Q is not an accurate measure of the bulk capacitance. In the non-ideal case, a distinct value for the bulk capacitance cannot be obtained because of the frequency dependence of the di-

TABLE 1. Impedance relations for some basic circuit elements, derived from the impedance function of a constant phase element given in Eq 2.

Circuit Element	n-value	Z(CPE)		Constant
resistor	0	B	Z(R)	$B = R$
capacitor	1	$-jB/\omega$	Z(C)	$B = C^{-1}$
inductor	−1	$j\omega B$	Z(L)	$B = L$
Warburg diffusional element	0.5	$B(1 - j)(2\omega)^{-1/2}$	Z(W)	$B = Q^{-1}$

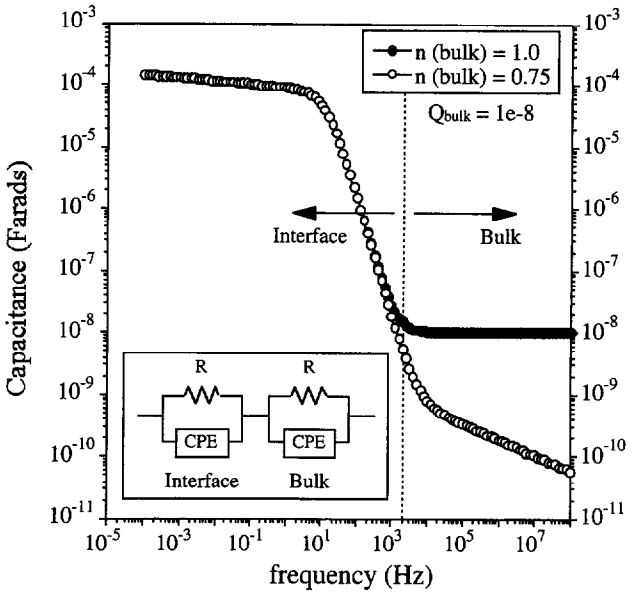

FIGURE 3. The capacitive response of the inset equivalent circuit with bulk *n*-values of 1 and 0.75. The two parallel resistor-CPE circuit combinations represent bulk and interfacial impedance responses.

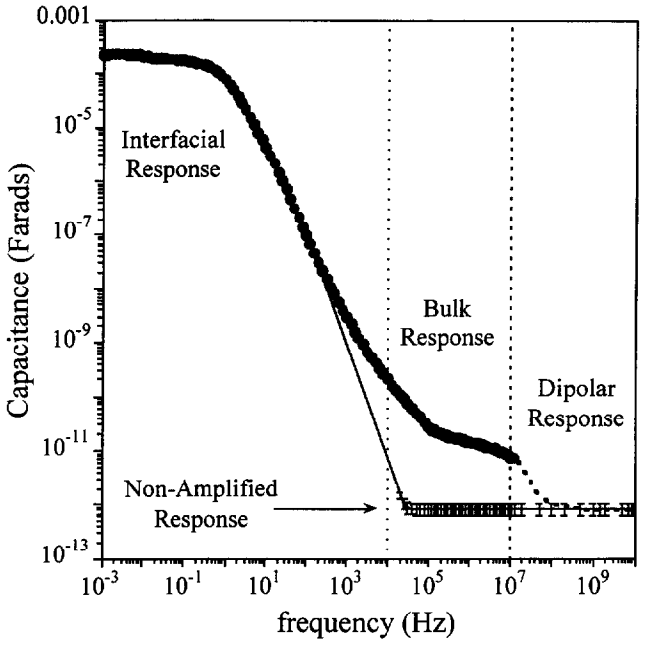

FIGURE 4. Extended spectrum for the dielectric behavior of a neat OPC paste of w/c = 0.4 at a hydration time of 20 hr (ϕ = 0.4 ± 0.05). The behavior above 10^7 Hz is taken from Ref 22.

electric response. The bulk capacitance for this simulation can be estimated as having a value in the 10^{-10}F range, as can be seen in the figure. The *Q*-value obtained by NLLS fitting of the lower curve (10^{-8}) is not a good approximation of the true bulk capacitance ($\approx 10^{-10}$), being in error by more than an order of magnitude.

Numerical fitting errors cannot completely account for the observed dielectric behavior at intermediate frequencies (10^4–10^7 Hz) in cement-based systems. Figure 4 shows the dielectric response as a function of frequency of a w/c = 0.4 OPC paste at 20 hours of hydration. Various mechanisms are indicated in the extended spectrum with an electrode interfacial response at lower frequencies (mHz–Hz), a water dipolar response at the highest frequencies (MHz–GHz), and a bulk response in the intermediate frequency range (kHz–MHz) [20]. The highest frequency capacitive response is beyond the measurement range of most impedance equipment, which are usually limited to below 30 MHz. Recent reports in the literature have provided this high frequency information, measured using microwave frequency analyzers [21–23]. Because aqueous electrolytes have resonant frequencies in the GHz range, these measurements provide information on the dielectric behavior of the pore solution in cement-based materials. Figure 5 shows the results of dielectric measurements made at 10 GHz for several porous systems as a function of the volume fraction of porosity they contain

TABLE 2. Circuit element values assumed in the capacitance vs. frequency simulations shown in Figure 3.

	Resistance	Q-value	n-value
Interface	10^5 Ω	10^{-4}	0.95
Bulk	150 Ω	10^{-8}	1.0 and 0.75

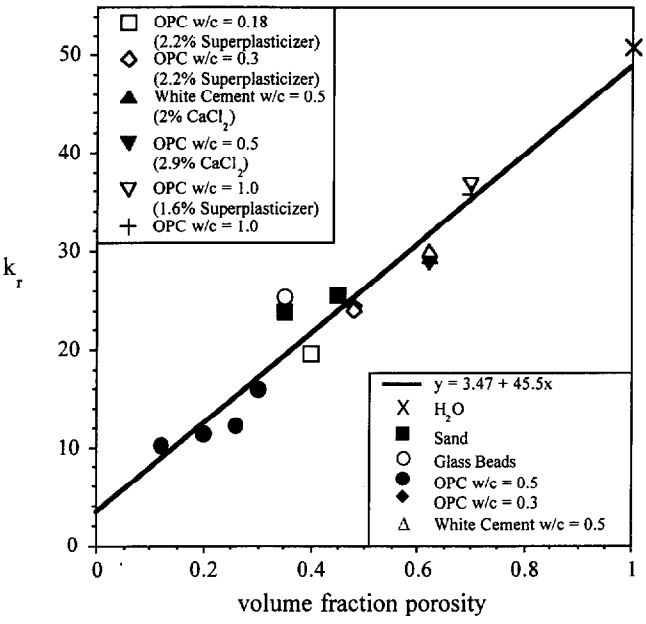

FIGURE 5. Dielectric constant values collected at 10 GHz for various porous systems vs. their volume fraction of porosity (after Brodwin).

[24,25]. The GHz frequency capacitance values appear to depend only on the amount of free (capillary) water in the system, in validation of Eq 1.

Between the dipolar (GHz) and interfacial (sub-Hz) plateaus in Figure 4, there is clear indication of an intermediate frequency (10^4–10^7 Hz) plateau. Capacitances in this frequency range fall typically one to two orders of magnitude higher than can be accounted for on the basis of the dipolar response of capillary pore water, based upon Eq 1 and the plot in Figure 5. In all subsequent plots, the capacitance-frequency behavior is examined over the 10^4–10^7 Hz frequency range and compared with the "non-amplified response," i.e., the capacitance based upon a reasonable range of free water contents and the relationship in Figure 5.

Dielectric Amplification

In the computer modeling work of Coverdale et al. [4], dielectric amplification could be obtained when complete or incomplete C-S-H gel phase barriers blocked the current flow between two adjacent capillary pores. In the present work, a physical model which simulated incomplete blockage between pores was constructed and tested for dielectric amplification.

Simplified Model of a Constricted Microstructure

The simplified experimental model of Figure 1 was used to simulate the effects of hydration on the electrical properties of cement paste microstructures. As hydration proceeds, constriction of the pore microstructure occurs in cement pastes as C-S-H gel is formed, which consumes free water and constricts passages in the capillary pore network [26,27]. This constriction of the capillary pores makes fluid and current flow more difficult [7], and these impediments are simulated by the polycarbonate barriers in the experimental model.

Figure 6 shows the Nyquist and capacitance behavior of three different polycarbonate configurations; one without a constricting barrier and two with barriers of different thicknesses but identical hole diameters. When a barrier is present, the Nyquist plot shows a second arc which implies series behavior. The presence of two arcs in the complex plane is observed only when the constricting hole in the barrier is within a certain size range and can be understood with the aid of the equivalent circuits in Figure 7. When the hole is small, the capacitance of the electrolyte within the hole is much less than that of the barrier itself, and the barrier capacitance dominates the response. For the polycarbonate model, the size restrictions needed to produce two arcs in the complex plane can be described by the relation:

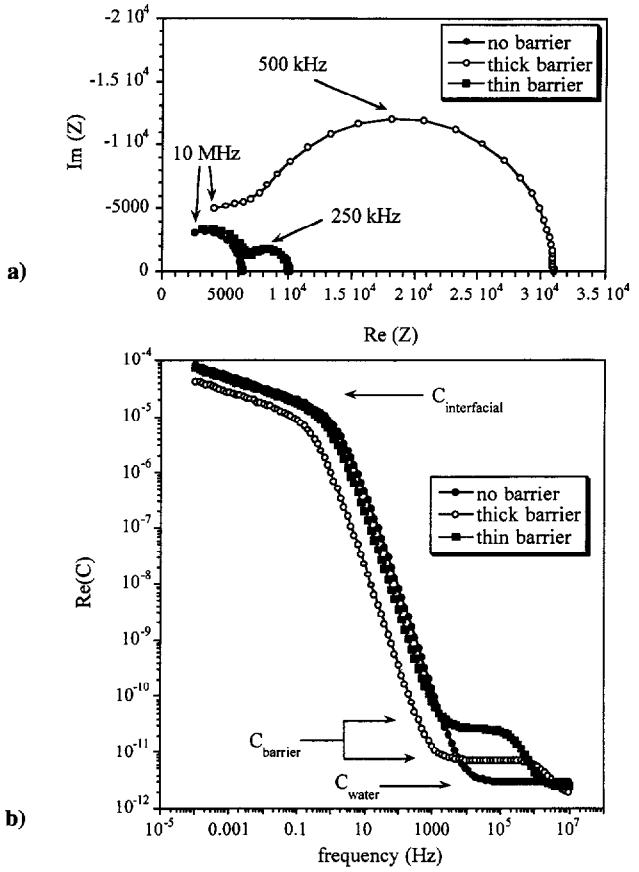

FIGURE 6. **a)** Nyquist and **b)** Capacitance vs. frequency plots for the simple polycarbonate experiments used to model the behavior of other constricted microstructures.

$$\frac{\rho_b}{\rho_e} \gg \frac{A-a}{a} \gg \frac{k_r^e}{k_r^b} \tag{8}$$

where ρ_b and ρ_e are the resistivities of the barrier and electrolyte respectively, k_r^b and k_r^e are the dielectric constants of the barrier and electrolyte materials, A is the area of the barrier, and a is the area of the hole. Therefore, as long as the ratio of the barrier and hole areas is within this range, the equivalent circuit in Figure 7a is reduced to the circuit in Figure 7b, giving rise to two arcs in the complex impedance plane. It should be stated, however, that this circuit model is not strictly correct. The high frequency arc, to the left of the Nyquist plot in Figure 6a, is affected by current spreading at the point of constriction. In essence, the current flow near the hole is perturbed so that the sampled "pore" area is less than the geometric area (A), and resistance values for the electrolyte (R_{water}) are larger than expected. This effect becomes more pronounced as the microstructure becomes more constricted. (Note: The RC elements of the polycarbonate side walls are ignored for the moment, but will become important in

Advn Cem Bas Mat
1997;5:41–48

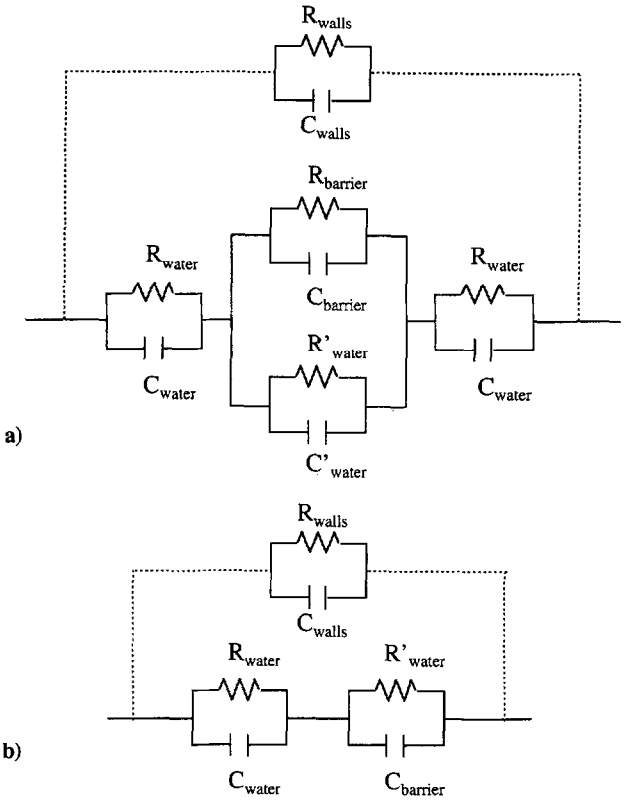

FIGURE 7. Equivalent circuit for the single barrier polycarbonate model. **a)** reduces to **b)** for small holes. Note that R_{water} represents a combination of the two side chambers of Figure 1 into a single element, likewise for C_{water}.

the discussion of cement pastes, especially during freezing and solvent exchange.)

This simple model of cement-based systems does not require the pore system to be depercolated, which was a major concern in the early modeling work of Coverdale et al. [4]. Percolation in any model concerning the microstructure of cement-based materials is important, because the pore network for most cementitious systems is continuous at early hydration times when dielectric amplification is at a maximum, and for many systems the pore network is continuous even at long hydration times [27]. It can be seen from Eq 8 that depercolation nullifies the circuit model of Figure 7b. As the area of the hole goes to zero, the barrier becomes a series component in the circuit, greatly increasing the resistance of the system. It will therefore become important to include the C-S-H gel phase in the equivalent circuit models of depercolated cementitious systems.

Figure 6b illustrates how the constriction of electrical current flow in the experimental models has an amplifying effect on the bulk capacitance of the system. When the barrier is thin, the voltage drop across it produces a large, amplified capacitance. As thicker barriers are used, the capacitance decreases analogously to an increase in plate separation in a parallel plate capacitor. The amplified capacitance is the capacitance of the barrier above the expected capacitance of the system without a barrier. This response is similar to that described for cement paste during hydration, as in Figure 4. As an analogy, C-S-H barriers can be thought to form in the pore network at early times, causing an increase in the bulk capacitance due to the constriction of the pore network and the voltage drop across C-S-H barriers. As hydration proceeds, these barriers thicken, causing the capacitance to decrease. At long times, the hydration reaction slows and the bulk capacitance reaches a plateau.

Experimental Results

To test the validity of the barrier/hole analogy, theoretical results from Eq 1 were compared with experimental observations of real cement paste systems. Figure 8 shows how the capacitance of a neat OPC paste of w/c = 0.4 changes with hydration time. As with the simple microstructural model presented above, the capacitance decreases with time, presumably due to the thickening of the C-S-H barriers. An implication of this microstructural model is that dielectric amplification should be more pronounced when the system is more open and fewer barriers are present. In other words, the same voltage is being dropped across shorter distance, i.e., higher capacitances can be expected. A higher water content in a cement paste produces larger capillary

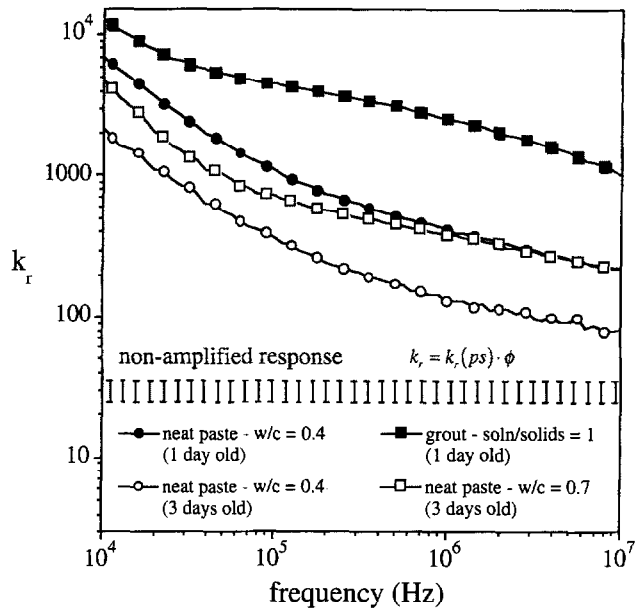

FIGURE 8. Capacitance vs. frequency plot for various cement-based systems, comparing hydration times (at fixed w/c ratio) and w/c ratios (at fixed hydration time). ($\phi = 0.4 \pm 0.05$)

pores and creates a more open microstructure with fewer barriers [26,27]. To further test the model, pastes with various w/c ratios were compared. Figure 8 also shows how the dielectric constant vs. frequency responses of a w/c = 0.7 OPC paste, and a grout with a solution:solids ratio of approximately 1.0 [28] compare with a paste of w/c = 0.4 at the same hydration times. It can be seen that dielectric amplification is more pronounced at high w/c ratios, as anticipated when larger pores (fewer barriers) are present.

The C-S-H gel phase may itself be a dielectrically amplified microstructure, dominating the electrical response of cementitious systems in which the larger capillary pore network is nearly consumed or is highly tortuous. This is illustrated by the relatively high capacitances evident for cement pastes at long times when the free water is consumed and the volume fraction of capillary porosity is near zero [1]. This additional level of amplification can be seen more clearly in freezing and solvent exchange experiments.

Figures 9 and 10 show the effects of freezing and solvent exchange, respectively, on the capacitive behavior of cement pastes. During freezing (Figure 9), a precipitous drop occurs in the dielectric constant at approximately −5°C, followed by a more gradual decline as the temperature is decreased [14]. The precipitous drop can be explained by the freezing of the free water in capillary pores, eliminating the conductive large pores/constrictions (R_{water}, $R'_{water} \rightarrow \infty$ in Figure 7b). What remains is the dielectric response of the continuous C-S-H product phase, i.e., the side walls in Figure 7.

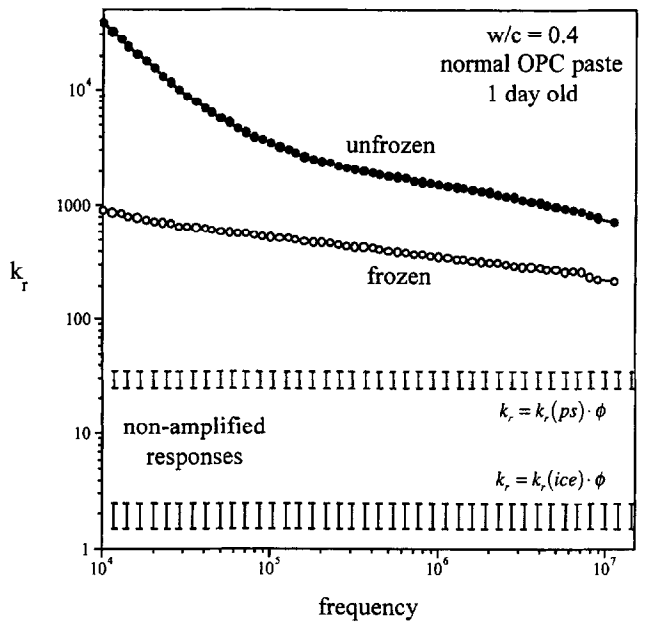

FIGURE 9. Dielectric constant vs. frequency plots for a frozen and unfrozen neat OPC paste of w/c = 0.4 at 1 day of hydration (ϕ = 0.4 ± 0.05)

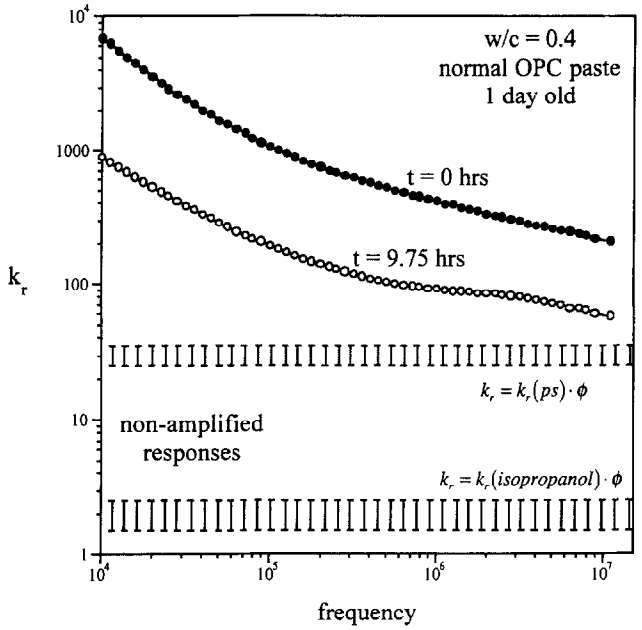

FIGURE 10. Dielectric constant vs. frequency plots for a neat OPC paste of w/c = 0.4 at 1 day of hydration, before exchange and after nearly 10 hours of solvent exchange with isopropanol. (ϕ = 0.4 ± 0.05)

The gel pores, being on a much smaller size scale, keep the gel water from freezing until lower temperatures are reached. Figure 9 shows that the capacitance of the frozen system is still higher than the capacitance predicted by Eq 1. This implies that there is a residual dielectric amplification associated with C-S-H gel, possibly of similar origin to the amplification in the capillary pore system, but on a smaller scale.

A similar explanation can be made concerning the isopropanol exchange of the capillary porosity in cement pastes. Because isopropanol has a large molecular size relative to water, it is thought to exchange only the capillary water in the system, because the gel pores are smaller than the solvent molecules [11]. As in freezing, solvent exchange greatly reduces the conductivity of this capillary pore network (R_{water}, $R'_{water} \rightarrow \infty$ in Figure 7b). Figure 10 shows that the system capacitance after solvent exchange is still large relative to the non-amplified response, implying that C-S-H gel is a dielectrically amplified microstructure. This residual level of amplification can be virtually eliminated upon solvent exchange with methanol, a much smaller molecule than isopropanol which is thought to more fully exchange gel pores in addition to capillary pores [11,29].

Conclusions

The impedance spectra of cement pastes at early ages of hydration show evidence of dielectric amplification, i.e.,

dielectric constants larger than can be accounted for on the basis of water dipolar response. This is best seen in plots of capacitance vs. frequency in the 10^4–10^7 Hz range. Because of arc depression, non-linear least squares fitting with equivalent circuits involving constant phase elements can lead to erroneously high "capacitance" values. This problem is avoided by using capacitance vs. frequency plots.

A simple physical model of the "constricted" pore structure of cement pastes consists of reservoirs (pores) separated by a barrier (C-S-H gel) with a hole to retain percolation. The resulting capacitance-frequency behavior is similar to that of cement pastes, i.e. there is substantial dielectric amplification in the 10^4–10^7 Hz range. The model shows that dielectric amplification is inversely proportional to the barrier thickness, and that the pore network need not be depercolated, as predicted by Coverdale et al. [4].

Dielectric amplification in cement pastes can be explained on the basis of the physical model. Depending on w/c ratio and degree of hydration, capacitance values up to two orders of magnitude larger than what can be accounted for by water dipole relaxation can be obtained. Factors which increase pore size (e.g., w/c ratio) or decrease product layer thicknesses (short times of hydration) lead to higher dielectric constants. The dielectric amplification arising from the constricted pore network can be reduced by preferentially freezing or solvent exchanging the capillary pores. In these cases, the residual dielectric amplification (upon freezing or solvent exchange) argues for dielectric amplification in the C-S-H gel phase, albeit on a finer scale.

Acknowledgments

This work was supported by the National Science Foundation through the Science and Technology Center for Advanced Cement-Based Materials under grant. DMR–91–20002. The authors also wish to gratefully acknowledge Donggy Sohn and Professor M.E. Brodwin for beneficial advice and discussions.

References

1. Christensen, B.J.; Coverdale, R.T.; Olson, R.A.; Ford, S.J.; Garboczi, E.J.; Jennings, H.M.; Mason, T.O. *J. Am. Ceram. Soc.* **1994,** *77,* 2789–2804.
2. Christensen, B.J.; Mason, T.O.; Jennings, H.M. *J. Am. Ceram. Soc.* **1992,** *75,* 939–45.
3. Coverdale, R.T.; Christensen, B.J.; Jennings, H.M.; Mason, T.O.; Bentz, D.P.; Garboczi, E.J. *J. Mat. Sci.* **1995,** *30,* 712–719.
4. Coverdale, R.T.; Christensen, B.J.; Mason, T.O.; Jennings, H.M.; Garboczi, E.J. *J. Mat. Sci.* **1994,** *29,* 4984–4992.
5. Gu, P.; Xie, P.; Beaudoin, J.J.; Brousseau, R. *Cem. Concr. Res.* **1992,** *22,* 833–840.
6. Gu, P.; Xie, P.; Beaudoin, J.J.; Brousseau, R. *Cem. Concr. Res.* **1993,** *23,* 157–168.
7. Garboczi, E.J. *Cem. Concr. Res.* **1990,** *20,* 591–601.
8. Xu, Z.; Gu, P.; Xie, P.; Beaudoin, J.J. *Cem. Concr. Res.* **1993,** *23,* 1007–1015.
9. Xu, Z.; Gu, P.; Xie, P.; Beaudoin, J.J. *Cem. Concr. Res.* **1993,** *23,* 853–862.
10. Brantervik, K.; Niklasson, G.A. *Cem. Concr. Res.* **1991,** *21,* 496–508.
11. Moss, G.M.; Christensen, B.J.; Mason, T.O.; Jennings, H.M. *ACBM* Vol. 4, 68–75 (1996).
12. McLachan, D.S.; Blaszkiewicz, M.; Newnham, R.E. *J. Am. Ceram. Soc.* **1990,** *73,* 2187–2203.
13. Ford, S.J.; Mason, T.O.; Christensen, B.J.; Coverdale, R.T.; Jennings, H.M.; Garboczi, E.J. *J. Mat. Sci.* **1995,** *30,* 1217–1224.
14. Olson, R.A.; Christensen, B.J.; Coverdale, R.T.; Ford, S.J.; Moss, G.M.; Jennings, H.M.; Mason, T.O.; Garboczi, E.J. *J. Mat. Sci.* **1995,** *30,* 5078–5086.
15. Scribner Associates *Z60/ZVIEW for Windows;* Charlottesville, VA 22901, 1994.
16. Boukamp, B.A. *Equivalent Circuit;* University of Twente: Netherlands, 1988.
17. Boukamp, B.A. *Solid State Ionics* **1986,** *20,* 31–44.
18. Macdonald, J.R. *Impedance Spectroscopy: Emphasizing Solid Materials and Systems;* John Wiley & Sons: New York, 1987.
19. Cole, K.S.; Cole, R.H. *J. Chem. Phys.* **1941,** *9,* 341–351.
20. Ford, S.J.; Mason, T.O. *Techniques to Assess the Corrosion Activity of Steel Reinforced Concrete Structures* **1995,** ASTM STP 1276.
21. Gu, P.; Beaudoin, J.J. *J. Mat. Sci. Lett.* **1995,** *14,* 613–614.
22. Gu, P.; Beaudoin, J.J. *J. Mat. Sci. Lett.* **1996,** *15,* 182–184.
23. Zhang, X.; Ding, X.Z.; Ong, C.K.; Tan, B.T.G.; Yang, J. *J. Mat. Sci.* **1996,** *31,* 1345–1352.
24. Chang, J.T. *Ph. D. Thesis;* Northwestern University, **1995.**
25. Brodwin, M.E., **1996,** manuscript in preparation.
26. Taylor, H.F.W. *Cement Chemistry;* Academic Press: San Diego, CA, 1990.
27. Mindess, S.; Young, J.F. *Concrete;* Prentice-Hall, Inc.: Englewood Cliffs, NJ, 1981.
28. Olson, R.A.; Tennis, P.D.; Bonen, D.; Christensen, B.J.; Jennings, H.M.; Mason, T.O.; Brough, A.R.; Young, J.F. *J. Hazard. Mat.* **1996,** in press.
29. Mikhail, R.S.; Selim, S.A. *Adsorption of Organic Vapors in Relation to the Pore Structure of Hardened Portland Cement Pastes;* Powers, T.C. ed.; National Research Council: Washington, D.C., 1996; pp. 123–134.